60 GHz antenna measurement setup using a VNA without external frequency conversion

Popa, Paula Irina; Pivnenko, Sergey; Nielsen, Jeppe Majlund; Breinbjerg, Olav

Published in:
Proceedings of the 36th Annual Symposium of the Antenna Measurement Techniques Association (AMTA)

Publication date:
2014

60GHz Antenna Measurement Setup Using a VNA without External Frequency Conversion

Paula Irina Popa, Sergey Pivnenko, Jeppe M. Nielsen, Olav Breinbjerg
Department of Electrical Engineering, Technical University of Denmark
Ørsteds Plads, 348, 2800 Kgs. Lyngby, Denmark

***Abstract*—The typical antenna measurement system setup working above 20 GHz makes use of frequency multipliers and harmonic mixers, usually working in standard waveguide bands, and thus several parts need to be procured and interchanged to cover several frequency bands. In this paper, we investigate an alternative solution which makes use of a standard wideband VNA without external frequency conversion units. The operational capability of the Planar Near-Field (PNF) Antenna Measurement Facility at the Technical University of Denmark was recently extended to 60 GHz employing an Agilent E8361A VNA (up to 67 GHz). The upgrade involved procurement of very few additional components: two cables operational up to 65 GHz and an open-ended waveguide probe for tests in U-band (40-60 GHz). The first tests have shown good performance of the PNF setup: 50-60 dB dynamic range and small thermal drift in magnitude and phase, 0.06 dB and 6 degrees peak-to-peak deviations over 4 hours. A PNF measurement of a 25 dBi Standard Gain Horn was carried out and the results were compared to those from the DTU-ESA Spherical Near-Field Facility with a good agreement in the validity region. Uncertainty investigations regarding cable flexing effects at 60 GHz have shown that these introduce an uncertainty of about 0.02 dB (1 sigma) around the main beam region indicating a very good performance of the PNF setup.**

I. Introduction

The interest in the millimeter wave spectrum (30-300 GHz) has increased lately due to a number of benefits which it brings in wireless communications systems: operation in an unlicensed band, wide available bandwidth and large transmission capacity of information, secure communication and frequency reuse due to special propagation characteristics of mm waves (oxygen and water absorption), miniaturization and ease of multiple elements integration. Antenna tests at frequencies above 20 GHz typically make use of frequency multipliers and harmonic mixers in order to reduce loss in long cables and thus improve the dynamic range of the measurement system. These frequency conversion devices usually work in standard waveguide bands and thus several parts need to be procured and interchanged to cover several frequency bands. It is also noted that changing characteristics of a flexing cable in e.g. Planar Near-Field (PNF) setup have increasing effect at higher frequencies due to increasing electrical length and usually the phase variation becomes unacceptably large. Thus, various compensation and correction approaches were proposed and investigated over the years [1], [2], [3], [5], [9].

In this paper, we report an alternative solution which involves a standard wideband VNA without external frequency conversion units. The operational capability of the PNF Antenna Measurement Facility at the Technical University of Denmark (DTU) was recently extended to 60 GHz employing an Agilent E8361A VNA working up to 67 GHz and few additional hardware components: two cables operational up to 65 GHz and an open-ended waveguide probe for tests in U-band (40-60 GHz). The performance of the upgraded measurement setup was analyzed through a series of tests including the achieved dynamic range, typical thermal drift, and effects of the flexing cable. Finally, a full scan PNF measurement of a 25 dBi Standard Gain Horn (SGH) was carried out and the results were compared with the reference result obtained at the DTU-ESA Spherical Near-Field Facility. Post-processing also included back projection of the PNF results to obtain the aperture field of the SGH. Since the magnitude and phase variations in mm-wave bands due to moving cable usually represent a serious problem, this effect was investigated in details. An uncertainty investigation on the cable flexing effect was carried out using measured magnitude and phase variations at 60 GHz and their influence on the far field results of the measured SGH are characterized in terms of the standard deviation.

II. Upgrade of the PNF Measurement Setup

The DTU PNF Antenna Measurement Facility is based on a 0.8 x 1.5 m^2 planar scanner developed in the 1990ies. The motor controllers and step motors from JVL [11] provide a xy-resolution of 0.0125 mm, while the scan plane planarity is estimated to be within a few tens of mm depending on the scan area. The PNF Antenna Measurement Facility is an educational tool used by students for courses and projects within the M.S.c.E.E. educational program at DTU.

During the past years the PNF Facility has undergone several upgrades including development of the control and data processing software in Matlab environment, use of a VNA controlled through GPIB and manufacturing of several probes. The latest upgrade carried out in the spring of 2014 included integration of the Agilent E8361A VNA, procurement of two cables with 1.85 mm connectors operational to 65 GHz (from Pasternack [10]) and manufacturing of an open-ended circular waveguide probe for U-band. The probe is based on a WR-19 waveguide Orthomode Transducer (OMT) from Millitech [12], but is currently used only in one polarization; the connection of the available waveguide switch is planned for the near future. The side view of the DTU PNF Facility is shown in Fig. 1.

In order to reduce the loss in the cables, the length of these was chosen to be as small as possible. The cable connecting

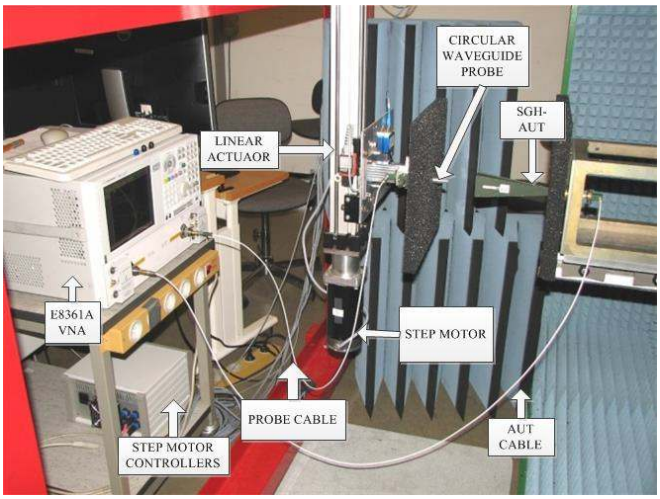

Fig. 1. DTU PNF measurement setup for 40-60 GHz

the VNA to the moving probe has the length of 120 cm, while the cable connecting the VNA to the AUT has the length of 150 cm, see Fig. 1. The maximum scan area for the probe used at 60 GHz is currently limited to some 200 x 220 mm^2. Thus the shape of the moving cable varies rather smoothly ensuring minimum changes in its electrical characteristics.

The return loss of the cables show values larger than 20 dB in the 40-60 GHz band and transmission loss is around 7 dB and 10 dB at 60 GHz for the short and long cables, respectively. The measured return loss of the probe is above 15 dB in the whole 40-60 GHz band.

III. First Tests in the 40-60 GHz Band

A series of simple tests were carried out to choose optimum parameters of the VNA and analyze the performance of the PNF measurement setup at 60 GHz.

A. System dynamic range

It is desired to have as large dynamic range as possible and thus the VNA measurement settings were optimized to reduce the noise, while keeping the measurement time small. The IF bandwidth was set to 1 kHz and the signal source power level was set to 2 dBm (maximum level around 60 GHz). For the setup consisting of the two cables and the probe described above, and a SGH with 25 dBi gain, the received power level was measured to be around -30 dBm, while the noise floor measured by disconnecting the AUT cable , was measured to be around -90 dBm. Therefore the system dynamic range of about 60 dB was obtained through the whole 40-60 GHz frequency range. With these VNA settings for 11 frequency points, a single line scan with 3 mm steps over the 200 mm range takes about 3.5 min. Depending on the gain of the measured antenna and number of the frequency points, the VNA settings can be changed either to improve the dynamic range or to reduce measurement time.

B. Drift

Thermal drift is one of the error sources in antenna measurements, and it is especially important for near-field measurements, which may take several hours depending on the electrical size of the measured antenna. A magnitude and phase drift test over 4 hours was performed measuring the signal level every minute; the results are shown in Fig. 2 and Fig. 3.

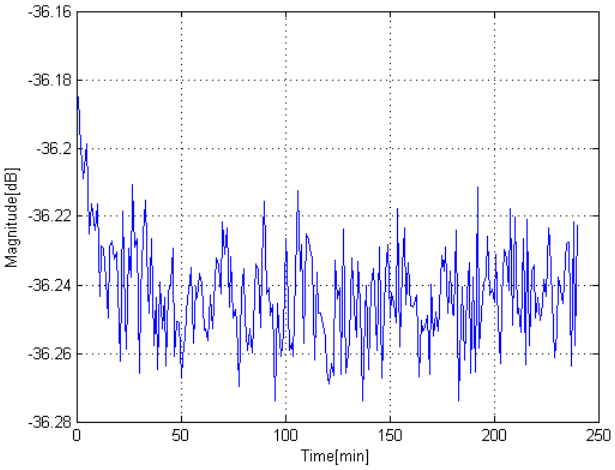

Fig. 2. Magnitude drift at 60 GHz over 4 hours

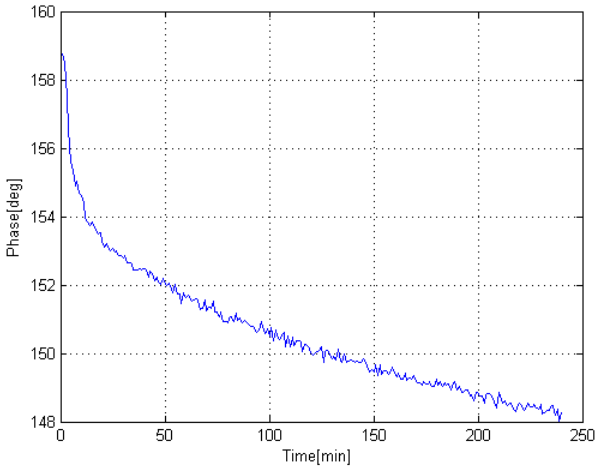

Fig. 3. Phase drift at 60 GHz over 4 hours

From Fig. 2 it is seen that excluding the initial 30 minutes of cable settling and warming up, the magnitude variation resembles noise with the peak to peak variation of about $\pm$0.03 dB. This peak to peak difference, however, corresponds to a noise floor at about -50 dB, thus the drift gives an additional contribution equivalent to decreasing the dynamic range by 10 dB. The phase drift, as seen from Fig. 3, has monotonic behavior changing with the rate of about 1.5° per

hour. For 60 GHz, this 1.5° phase change corresponds to a length change of merely 21 μm which is likely to have occurred due to temperature change during measurement (for a typical metal of 1m length this corresponds to 1°-2° of temperature change). For a long data acquisition it is necessary to keep the temperature very stable; in addition, reference point measurements and corresponding phase correction may be applied to reduce the phase drift.

C. Cable flexing

Since a major concern for the setup is the cable flexing effect on the measured results a series of tests were carried out in order to quantify magnitude and phase variations due to cable flexing. The transmission loss S_{21} between the probe and the SGH was measured by performing several identical horizontal line scans, each taking 3.5 minutes and the Equivalent Error Signal (EES) was calculated using (1) Section V; the results are shown in Fig. 4.

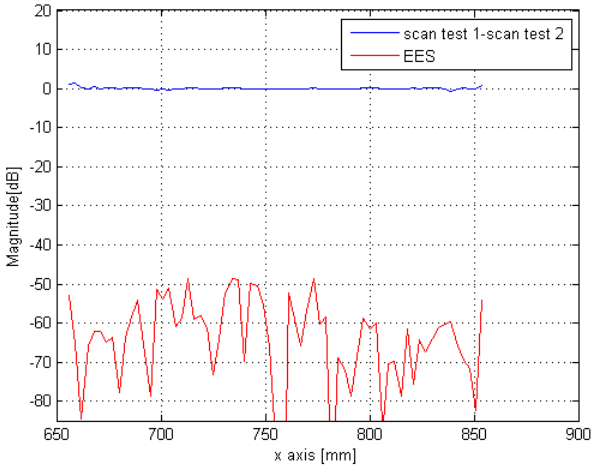

Fig. 4. Magnitude difference between two horizontal line scans and EES level at 60 GHz

The EES curve indicates a level around -49dB which causes a peak to peak deviation of 0.01dB (1 sigma). The results show small magnitude variations between repeated line tests, slightly exceeding the noise floor level of -50 dB.

To further analyze the magnitude and phase variations due to flexing cable, measurements of the reflection coefficient S_{22} were carried out with the cable connected to the moving OMT which was short circuited in the aperture. The measured magnitude and phase variations from 5 consecutive horizontal and vertical line scans each taking 3.5 minutes, are shown in Fig. 5 to Fig. 8.

It can be seen from Fig. 5 and Fig. 6 that the magnitude and phase from five sequential measurements along the horizontal scan axis are not identical. The first scan, and to some extent the second scan, obviously reflects a start-up problem and it can be disregarded. Hence the following analysis is based on the last 3 scans.

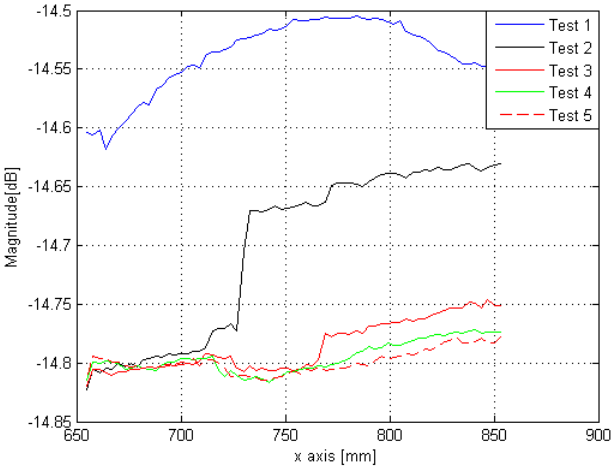

Fig. 5. Horizontal line scans at 60 GHz, magnitude of the reflection coefficient from the short-circuited OMT

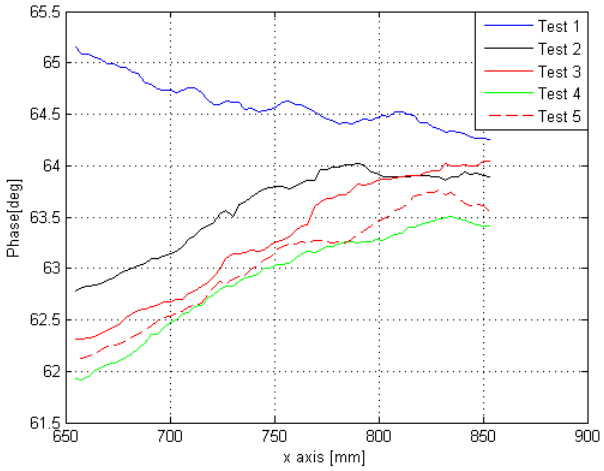

Fig. 6. Horizontal line scans at 60 GHz, phase of the reflection coefficient from the short-circuited OMT

The magnitude and phase absolute difference between the last three scans is less than 0.05 dB and around 1°. Within one horizontal line scan the peak to peak magnitude and phase variations show values around 0.07 dB and 1.7°.

Vertical line scans (Fig. 7 and Fig. 8) show maximum magnitude and phase variations of approximately the same order as for the horizontal scans. Also here the first scan is noticeably different from the remaining ones. The maximum deviations occur at the beginning and the end of the vertical line scan (Fig. 7, Fig. 8) with a good repeatability in the middle of the range with deviations of the order of hundredths of dB and tenths of degrees. Since the data show relatively small magnitude and phase variations and the results indicate rather a random behavior, no correction is applied to compensate for the cable flexing. Also, taking into account that the results shown are for the reflection coefficient, (not

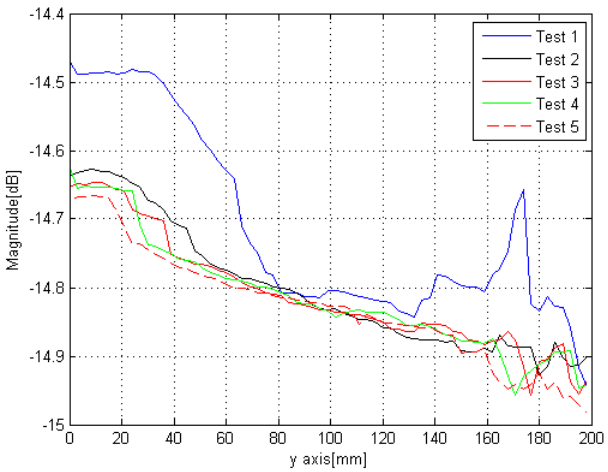

Fig. 7. Vertical line scans at 60 GHz, magnitude of the reflection coefficient from the short-circuited OMT

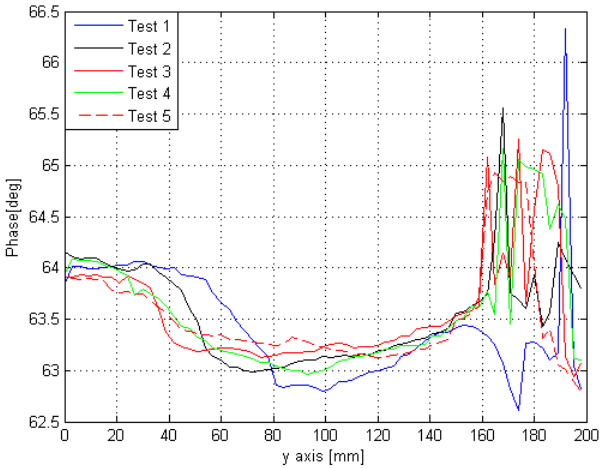

Fig. 8. Vertical line scans at 60 GHz, phase of the reflection coefficient from the short-circuited OMT

transmission coefficient) it can be assumed that the magnitude and phase deviations are only half of observed values for the transmission case. Therefore, it can be considered that the cable flexing effect on magnitude and phase stability is rather minor. In order to clarify how the observed magnitude and phase differences would affect the far field data, uncertainty investigations were performed as documented in Section V.

IV. SGH Measurement

A. PNF measurement of the SGH

Finally, a full-scan PNF measurement of a SGH with 25 dBi gain was carried out. The scan plane size was 220 x 200 mm^2 with the step size of 2.5 mm both along x- and along y-axes. The distance between the SGH aperture and the probe aperture was 30 mm, and with the SGH aperture dimensions of 30 x 40 mm^2, the angular validity region for the SGH far-field pattern was calculated to be $\pm 72°$ in the E-plane and $\pm 69°$ in the H-plane. The full-scan measurements were done first for the horizontal and then for the vertical probe polarizations with manual rotation of the probe. For 80x88 scan points, the duration of a full scan measurement for one polarization was around 8 hours. Probe correction was applied on the measured data.

B. Comparison with the reference results

Reference results for the radiation pattern of this SGH were obtained from measurements at the DTU-ESA Spherical Near-Field (SNF) Facility. A comparison of the co-polar and cross-polar patterns at 60 GHz in the E-plane (ϕ = 0°) and in the H-plane (ϕ = 90°) from the PNF Facility and from the SNF Facility are shown in Fig. 9.

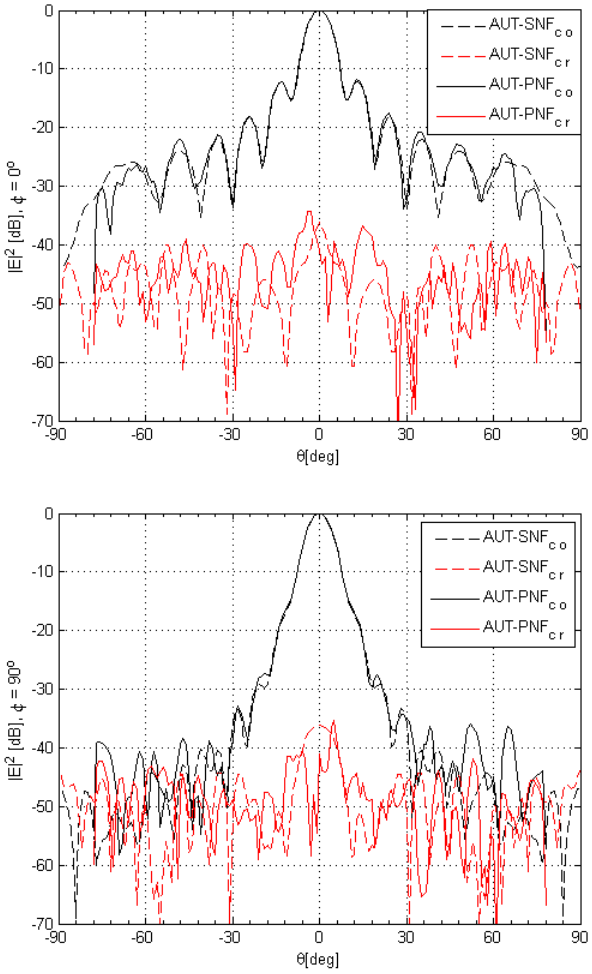

Fig. 9. SGH co-polar and cross-polar patterns at 60 GHz from the PNF setup and the SNF Facility: E-plane (top) and H-plane (bottom)

It is seen from Fig. 9, that the co-polar patterns show a good agreement within the main beam region, with some difference at the lower pattern levels. In the H-plane, at θ angles around 60° some rather large spikes are visible indicating the presence

of reflections in the PNF setup. The agreement in the cross-polar pattern is also rather good, even though the shape is quite different. It is noted that the cross-polar pattern is clearly asymmetric, which may also be explained by the room reflections in the PNF setup. The absorber treatment of the PNF setup is very limited, as can be seen from Fig. 1; it is planned in the near future to cover the scanner frame, the floor and ceiling with additional absorbers.

The other reasons for the asymmetry of the PNF pattern and difference between the PNF and SNF results can be the other sources of uncertainty, e.g. planarity of the PNF scan plane, effects of the drift and the flexing cable, scan plane truncation, and also incomplete probe correction. However despite of the long measurement time of a full scan, the comparison of the SNF and PNF shows a good agreement indicating rather a minor effect of the thermal drift on the PNF measured data. Concerning probe correction, the full-sphere probe pattern was accurately measured in the SNF Facility, but the channel balance for the probe orientations was assumed to be 1; the magnitude and phase difference due to bent cable may contribute to the SGH pattern uncertainty.

C. Back projection

In order to further verify the quality of the PNF measurement results the commercial software DIATOOL from TICRA was used to perform back projection of the radiated far field obtained from the PNF setup. The antenna aperture field was reconstructed on 10x10 cm surface. (Fig. 10). The amplitude of the tangential x and y components of the E-field at 60 GHz for the SGH are shown in Fig. 10 and the SGH aperture is represented by the black rectangle. The x-component shows the expected aperture field distribution typical for a SGH, while the y-component has the expected low level with some asymmetry; as explained above, this asymmetry is most probably caused by the room reflections of the PNF setup.

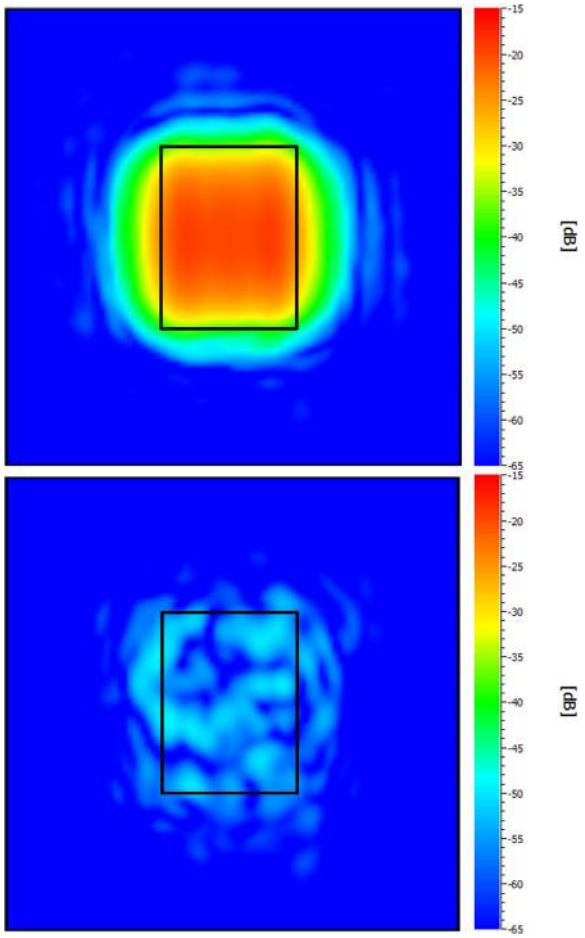

Fig. 10. Amplitude of the tangential E field at 60 GHz: x component (top), y component (bottom)

V. Flexing Cable Uncertainty Investigation

Since the major concern for the mm wave PNF measurement system are the cable signal magnitude and phase variations a detailed investigation on this uncertainty term is performed. To verify the cable flexing impact on the far field pattern, the raw near-field data was modified with values taken from the measured variations of the magnitude and phase of the reflection coefficient from the short-circuited OMT. The modified data was then processed to obtain the far field. As noted in Section IV, it can be assumed that the differences in magnitude and phase obtained from the measurements of the reflection coefficient are twice larger than those for the transmission coefficient. To investigate the cable magnitude and phase variations effect, the corresponding maximum difference between the measurements of the reflection coefficient was divided by 2, then added or subtracted to the magnitude and phase of the near field data and the obtained modified near-field data was transformed to the far field. Since for the vertical scans (y-axis) the variations of the cable in phase and magnitude are quite small in the center of the scan area region, the compensation was done only for the x-axis variations. For completeness, the near-field data modified with the full difference (not half) in magnitude and phase was analyzed as well.

For the obtained far-field pattern with modification and without modification (as measured), the EES was then calculated. The EES was obtained by subtracting the modified far-field pattern from the non-modified far-field pattern at 60 GHz in linear scale and by converting the result back to dB using the following formula:

$$EES = 20\log_{10}\left|\log_{10}^{-1}\left(S_{dB}/20\right) - \log_{10}^{-1}\left((S_{dB}+\delta_{dB})/20\right)\right| \quad (1)$$

Here, $(S_{dB} + \delta_{dB})$ indicates the modified far-field pattern and (S_{dB}) indicates the non-modified far-field pattern. The normalized patterns and the EES are shown in Fig. 11.

It can be seen from Fig 11 that the EES curve in the E-plane ϕ = 0° for the data modified with half value of the cable variations has a peak value around -48 dB and for the data modified with the full difference in magnitude and phase, a peak value around -42 dB. For the H-plane, ϕ = 90°, the EES

values are below -70 dB since for this plane no modification of the magnitude or phase was performed.

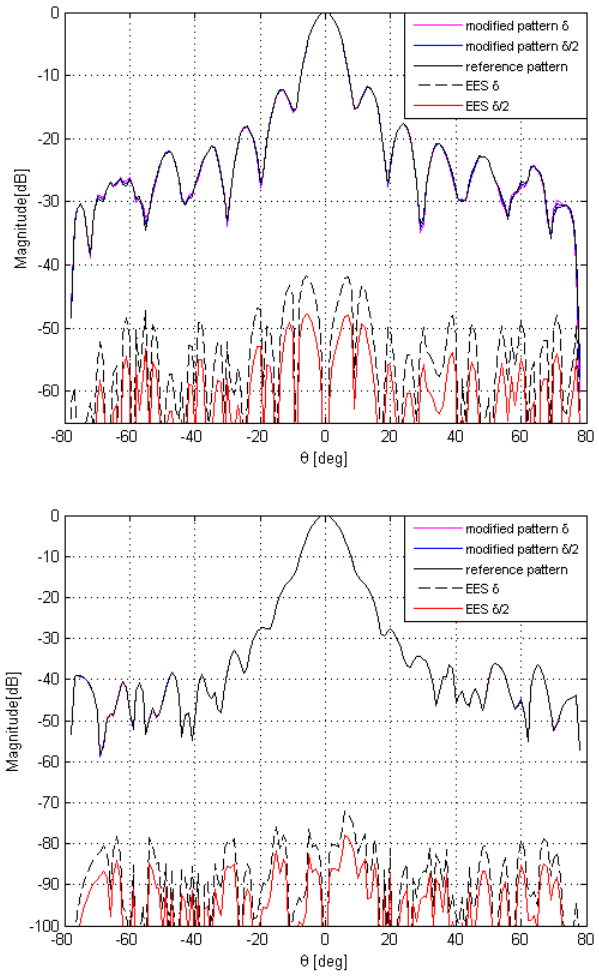

Fig. 11. Normalized radiation pattern with and without flexing cable correction and the EES levels for the half-value and full correction: ϕ = 0° plane (top) and ϕ = 90° plane (bottom)

The pattern standard uncertainty in dB due to the flexing cable is calculated by considering that the standard deviation is 1/3 of the corresponding peak to peak variation calculated with (1):

$$\Delta_{dB} = 20\log_{10}\left(\max\left(\log_{10}^{-1}\left(EES/20\right)\right) * 1/3 + 1\right) \quad (2)$$

In the E-plane (ϕ = 0°), the EES level of -42 dB causes the standard deviation of Δ_{dB} = 0.02 dB around the main beam peak, while the EES level of -48 dB causes the standard deviation of Δ_{dB} = 0.01 dB. The above calculations show, that the effects of the magnitude and phase variations due to the flexing cable are rather small.

VI. Conclusions

The PNF Antenna Measurement Facility at DTU was recently upgraded to 60 GHz without external frequency conversion devices. An Agilent E8361A VNA and few additional hardware components, two cables operational up to 65 GHz and U-band (40-60 GHz) open-ended waveguide probe, were employed. The series of tests has shown high performance of the upgraded measurement setup: 50-60 dB dynamic range, small magnitude and phase drift, and relatively small flexing cable effects. A comparison of the results from the full scan PNF measurement of a 25 dBi SGH with the reference results from the DTU-ESA Spherical Near-Field Facility has shown very good agreement in the co-polar pattern and reasonable agreement in the cross-polar pattern. A detailed investigation of the flexing cable effect on the obtained far-field pattern of the SGH has shown standard uncertainty between 0.01 - 0.02 dB. The overall results indicate that in the upgraded PNF setup the magnitude and phase variations due to flexing cable have a minor effect on the obtained far-field patterns.

It is planned to continue development of the PNF Facility by performing investigations on the scan plane planarity, applying appropriate absorbers around the scanner, improving the alignment capabilities of the antenna support and by employing a dual polarized probe in order to reduce the measurement time.

Acknowledgement

This work was supported by the H.C. Ørsted Foundation at the Technical University of Denmark.

References

[1] A.C. Newel, "Techniques for reducing the effect of measurement errors in near-field antenna measurements", *The Second European Conference on Antennas and Propagation EuCap*, 11-16 november, 2007.
[2] D. Janse van Rensburg, "A technique to evaluate the impact of flex cable phase instability on mm-wave planar near-field measurement accuracies", *ESA ESTEC Workshop on Antenna Measurements*, 1999
[3] S. McBride, D. Musser, "Results of a new RF cable correction method", *28th, Annual Meeting and Symposium of the Antenna Measurements Technique Association*, 2006
[4] S. Gregson, J. McCormick, C. Parini, "Principles of Planar Near-Field Antenna Measurements", London, United Kingdom, 2007
[5] G. Eason, E. Evans, "Antenna measurement techniques", *Artech House*, Boston-London, pp. 85-93, pp. 153-157, 1990.
[6] A.C.Newell, "Error analisys techniques for planar near-field measurements", *IEEE transactions on antennas and propagation*, vol.36, no.6, june 1988
[7] J.E. Hansen, "Spherical Near Field Antenna Measurements", *Peter Peregrinus Ltd.*, London, United Kingdom, 1988
[8] D. Slater, "Near-Field Antenna Measurements", *Artech House Inc.*, 1991
[9] D.W. Hess, "Principle of three-cable method for compensation of cable variations", *AMTA Symposium Digest*, pp 10-26-10-31, Columbus,OH,1992
[10] Pasternack Enterprises, Inc. www.pasternack.com
[11] JVL Industri Elektronik A/S, www.jvl.dk
[12] Millitech Inc., http://www.millitech.com